Jia *et al.*
Chinese Journal of Mechanical Engineering (2024) 37:13
https://doi.org/10.1186/s10033-024-00990-1

Chinese Journal of Mechanical Engineering

ORIGINAL ARTICLE

Open Access

Tribological Behaviors of Electroless Nickel-Boron Coating on Titanium Alloy Surface

Yao Jia[1], Jianping Lai[1], Jiaxin Yu[1*], Huimin Qi[1], Yafeng Zhang[1] and Hongtu He[1]

Abstract

Titanium alloys are excellent structural materials in engineering fields, but their poor tribological properties limit their further applications. Electroless plating is an effective method to enhance the tribological performance of alloys, but it is difficult to efficiently apply to titanium alloys, due to titanium alloy's strong chemical activity. In this work, the electroless Nickel-Boron (Ni-B) coating was successfully deposited on the surface of titanium alloy (Ti-6AL-4V) via a new pre-treatment process. Then, linearly reciprocating sliding wear tests were performed to evaluate the tribological behaviors of titanium alloy and its electroless Ni-B coatings. It was found that the Ni-B coatings can decrease the wear rate of the titanium alloy from 19.89×10^{-3} mm^3 to 0.41×10^{-3} mm^3, which attributes to the much higher hardness of Ni-B coatings. After heat treatment, the hardness of Ni-B coating further increases corresponding to coating crystallization and hard phase formation. However, heat treatment does not improve the tribological performance of Ni-B coating, due to the fact that higher brittleness and more severe oxidative wear exacerbate the damage of heat-treated coatings. Furthermore, the Ni-B coatings heat-treated both in air and nitrogen almost present the same tribological performance. The finding of this work on electroless coating would further extend the practical applications of titanium alloys in the engineering fields.

Keywords Electroless coating, Titanium alloy, Tribology, Wear, Heat treatment, Nanoindentation

1 Introduction

Titanium alloys are considered remarkable structural materials in the engineering fields due to their excellent properties, such as low density and high strength-to-weight ratio. However, low hardness and poor tribological properties limit the scope of their applications [1]. Till date, several traditional treatment techniques have been employed to improve the tribological properties of titanium alloys. However, these conventional methods inevitably induce other defects on the surface of titanium alloys [2–4]. For instance, Wagner [2] reported that sand-blasting can cause dislocation and macro residual stresses because of the plastic deformation and atomic stacking. Also, Weng et al. [3] found that laser cladding produced excessive residual stresses due to high heating and cooling rates during the cladding process. Moreover, laser cladding introduces cracks and pores in the laser cladding layer, which reduce the improvement efficiency of titanium surface properties. On the other hand, thermal spraying can only coat the region which the torch or gun can "see" because of the line-of-sight nature of deposition processes [4]. This shortcoming makes it challenging to control the interface bonding between the resultant coating and substrate material.

Electroless plating does not require an external power supply, and the electroless Ni-B coating exhibits some excellent characteristics such as high density, fine grains, uniform thickness, low porosity, and good wear resistance [5–7], which make it to be an ideal surface modification technology. Electroless Ni-B coatings can be deposited on several metal substrates, such as stainless

*Correspondence:
Jiaxin Yu
yujiaxin@swust.edu.cn
[1] Key Laboratory of Testing Technology for Manufacturing Process in Ministry of Education, State Key Laboratory of Environment-Friendly Energy Materials, Southwest University of Science and Technology, Mianyang 621010, China

steel [6], pure copper [6], magnesium alloy [8] and lower carbon steel [9, 10], and the resultant coatings demonstrate excellent mechanical and tribological properties. Correa et al. [8] reported that the wear rate of electroless Ni-B coating was lower than the magnesium alloy, by roughly two orders of magnitude. Arias et al. [9] revealed that the friction coefficient of heat-treated electroless Ni-B coating was only half of the low carbon steel substrate, which was attributable to the cauliflower morphology of electroless coating and boron acting as a solid lubricant. Therefore, the electroless Ni-B coating is expected to greatly prevent the wear of titanium alloy, once it could be successfully deposited on the titanium alloy's surface. However, as the chemical activity of titanium alloys is extremely strong, a thin oxide film readily forms on their surface when exposing to air, which reduces the bonding strength between the coating and substrate, and hinders the deposition of the coating [11]. The deposition of Ni-B coating on titanium alloys is much more difficult as compared to other common alloys. Therefore, few studies have focused on the deposition technology and tribological performance of electroless Ni-B coating on titanium alloys. Developing a new pre-treatment process that can achieve deposition of electroless Ni-B coating on titanium alloy has become a pressing need. Simultaneously, it is necessary to understand how Ni-B coating can improve the wear resistance of titanium alloy.

After the Ni-B coating deposition, its crystal phase structure was affected by heat treatment process [12]. The as-plated Ni-B coating has been reported to be an amorphous structure [6, 7]. An appropriate heat treatment can induce crystallization and grain growth of coating, which would influence its mechanical and tribological properties. Krishnaveni et al. [7] found that the hardness of electroless Ni-B coating was increased from 570 HV_{100} to 908 HV_{100} after heat treatment at 450 ℃. Mukhopadhyay et al. [13] reported that the Ni-B coating deposited on AISI 1040 steel substrate presented a better wear resistance and lower friction coefficient when heat-treated at 300 ℃, compared to 100 ℃ and 500 ℃. Shajari et al. [14] found that the wear mechanism of Ni-B coating on nickel aluminum bronze transformed from adhesive wear to abrasive wear, as the heat treatment temperature increased. Besides, the heat treatment atmosphere also affected the mechanical properties of coatings. For instance, Vitry et al. [15] reported that the heat treatment in an ammonia-based atmosphere resulted in the outer layer of Ni-B coating with poor mechanical properties. In spite of these studies, the effects of heat treatment on the tribological properties of electroless Ni-B coating on titanium alloy have not been completely addressed.

In this study, an electroless Ni-B coating was first deposited on the surface of titanium alloy (Ti-6Al-4V) with a new pre-treatment process and then was heat-treated in air and nitrogen. Thereafter, tribological behaviors of titanium alloy and its electroless Ni-B coatings were investigated and compared to understand the mechanism of enhanced wear resistance of Ni-B coatings and to reveal the effect mechanism of heat treatment on the tribological properties of Ni-B coating.

2 Materials and Methods

2.1 Pre-Treatment of Titanium Alloy

Ti-6Al-4V titanium alloy (TC4) with the dimensions of 15×10×3 mm was used as the substrate material (provided by the Baoji Titanium Industry Company, China). First, use 320, 800, 100, 1500, 2000, 3000# SiC sandpapers in sequence to polish the substrates and obtain a uniform surface roughness. This step was followed by ultrasonic cleaning of the samples in acetone for 8 min and soaking in an alkaline bath of Na_2CO_3, NaOH, and Na_3PO_4 for 13 min at 85 ℃ to degrease them. Afterward, the samples were dipped in a solution of HF and HCl at room temperature (RT) for 2 min to further remove the oxide layer. The surfaces of samples were then activated (hydrogenating treatment) in an acidic solution for 65 min to form a hydride conversion film to prevent surface oxidation. During each above-mentioned pre-treatment step, three TC4 titanium alloy samples were treated simultaneously, and magnetic stirring at 500 r/min was used to minimize the fluctuations in ion concentration and prevent the local overheating [16]. In the interval between each step, the samples were flushed with distilled water to ensure that there was no residual solution on their surfaces. The concentrations of specific reagent, solution volume, and temperature during the pre-treatment process before plating Ni-B coating on TC4 titanium alloy are shown in Figure 1. Notably, three pieces of TC4 samples were treated simultaneously following the steps above and are considered as one set of samples.

2.2 Electroless Bath

After pre-treatment, three samples in one set were immersed in one 300 mLl electroless Ni-B plating bath at 90 ℃ to ensure that the bath loading was less than 50 dm^2/L. The components of electroless Ni-B plating bath are listed in Table 1. The above plating parameters were preliminarily designed based on Refs. [12, 13, 17–19]. Then, they were further optimized, such as adjusting the bath composition and concentration, to adapt the titanium alloy substrate. The pH of the solution was adjusted to above 12 using sodium hydroxide to prevent the hydrolysis of sodium borohydride and spontaneous formation of nickel boride (Ni_2B) in the aqueous

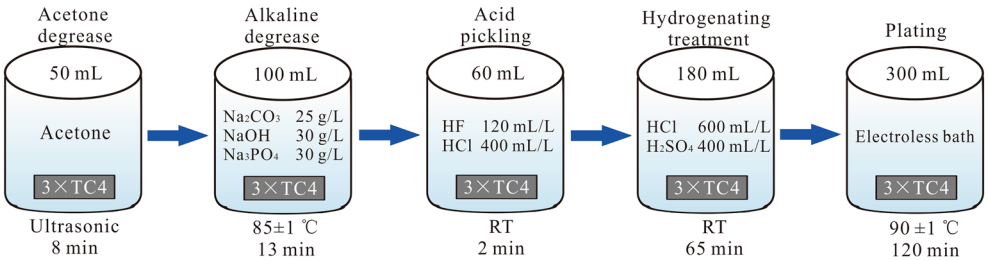

Figure 1 The pre-treatment flow diagram before plating Ni-B coating on TC4 titanium alloy

Table 1 The components of electroless Ni-B plating bath

Bath composition	g/L
Nickel chloride ($NiCl_2$)	25.00
Sodium hydroxide (NaOH)	30.00
Ethylenediamine ($C_2H_4(NH_2)_2$)	55.00
Sodium borohydride ($NaBH_4$)	0.80
Lead nitrate ($Pb(NO_3)_2$)	0.01

solution [20]. During electroless plating, the plating bath was continuously stirred at a speed of 500 r/min by a magnetic stirring apparatus. A fresh electroless plating bath was employed for each electroless plating to avoid any variation in the composition of plating bath during long-term storage. Notably, a double bath plating system was adopted, i.e., the plating bath was replaced by a fresh one after the first deposition of 2 h. The same deposition parameters were used in the double bath plating system to ensure the composition and thickness consistent in each layer of coating. With the consistent thickness, the dual-layer coating could present a better wear resistance than single-layer coating due to its better load bearing ability and crack resistance [21]. Moreover, dual-layer coating was reported to provide lower residual stresses and better adherence to metallic substrates [22].

2.3 Heat Treatment

The samples were heat-treated into a tube furnace at 350 ℃ for 3 h and naturally cooled to room temperature. Since 300–350 ℃ was found to be the crystallization temperature of Ni-B coating [23], 350 ℃ was chosen as the heat treatment temperature to transform coating structure from amorphous to crystal structure. Heat treatment for 3 h was chosen to ensure that the electroless Ni-B coating can crystallize. Moreover, the samples were heat-treated in air and nitrogen, respectively, to study the effect of heat treatment atmosphere on the tribological performance of electroless Ni-B coatings. There were three samples in one set, as shown in Figure 1. Two of them were heat-treated in air and nitrogen and labeled as air-treated and nitrogen-treated coating, respectively. The third one was the sample without heat treatment, which was labeled as as-plated coating. To ensure reproducibility, three sets of samples were prepared and treated, and the following chemical/mechanical tests were performed.

2.4 Chemical/Mechanical Analysis and Tribological Characterization

The morphology of coatings was observed using an optical microscope (BX51-P, Olympus, Japan), white light scanning profilometry (MFT3000, Rtec, San Jose, CA), and scanning electron microscopy (SEM, EVO18, Zeiss, Oberkochem, Germany). The elemental composition of as-plated Ni-B coating was analyzed via inductively coupled plasma-optical emission spectrometer (ICP-OES, 5110, Agilent, USA). The O content of heat-treated samples was analyzed using energy dispersive spectrum (EDS, EVO18, Zeiss, Oberkochem, Germany). The crystal phase structure of electroless Ni-B coatings was then analyzed using an X-ray diffractometer (XRD, D8 Focus Bruker, USA). Cu Kα radiation was used ($\lambda = 1.54187$ Å), operated at 40 kV and 40 mA, with an X'Celerator ultrafast detector based on real time multiple strip technology with Bragg-Brentano geometry. The scans were performed in the 2θ range from 3° to 90° at the step scan of 0.03° and 60 s per step in a continuous mode.

Moreover, nanoindentation was conducted to measure the mechanical properties of samples using nanoindenter (G200, Keysight, USA) equipped with a Berkovitch indenter. Before nanoindentation tests, the titanium alloy and its Ni-B coating samples were first polished to make their surface roughness less than 25 nm. In the nanoindentation test, the maximum indentation depth was ~1 μm on the Ni-B coatings, which was less than 10% of the coating thickness (~25 μm). It can not only avoid the interference of titanium alloy substrate but also the effect of surface defect caused by polishing on the hardness and modulus measurements. All tests were repeated 20 times and averaged to ensure reliability and repeatability. Furthermore, the micro-hardness of

unpolished samples was also measured, using the microhardness tester (HXD-1000TMC/LCD, China) equipped with a Vickers indenter, under a low load of 100 g, holding for 15 s. The binding force between coating and titanium alloy substrate was evaluated by ramping load scratching test using a diamond tip with a radius of 30 μm.

The tribological behavior of TC4 titanium alloy and Ni-B coatings was characterized using a linearly reciprocating ball-on-flat sliding tribometer (MFT3000, Rtec, San Jose, CA), as per ASTM G133-05 standard test method [24]. The samples served as the flat and Al_2O_3 balls (4 mm in diameter and 9 MOhs hardness) were used as counterbodies. The sliding distance was 3 mm, sliding speed was 2 mm/s, applied load was set as 10 N, and sliding time was 60 min. Before the wear tests, the samples and Al_2O_3 balls were ultrasonically cleaned in ethanol for 2 min and dried using dry air. To ensure the reproducibility of experimental results, each sample was subjected to at least three tribological tests. Then the all wear tracks on the samples were analyzed using white light scanning profilometry (Rtec, San Jose, CA) after cleaning the wear debris. The wear depth and volume were estimated based on the cross-sectional profile of the wear tracks. Moreover, the surface damage and elemental composition of wear tracks of samples were obtained using a scanning electron microscope (SEM) equipped with an energy dispersive spectrum (EDS) system. The wear tracks on Ni-B coatings were also analyzed using an X-ray photoelectron spectrometer (XPS, ESCALAB Xi+, ThermoFischer, USA) with an Al Kα source (1486.6 eV). The vacuum degree in the chamber was 8×10^{-10} Pa. All the survey scans were completed in 10 sweeps each with pass energies of 100 eV. The narrow scans had the step size of 0.05 eV, dwell time of 40–50 ms, and pass energy of 20 eV.

3 Characterization of Chemical and Mechanical Properties of Ni-B Coatings

3.1 Elemental Composition and Phase Structure of Electroless Ni-B Coatings

ICP analysis reveals that the as-plated Ni-B coating contains 91.51 wt% nickel, 7.80 wt% boron, and 0.69 wt% lead. It is proved that the electroless nickel boron coating has been successfully deposited on the surface of titanium alloy. After heat treatment, the air-treated coating was oxidized and an oxygen concentration of ~3 wt% was detected by EDS.

Figure 2 shows the XRD pattern of the three electroless Ni-B coatings. For the as-plated Ni-B coating, the typical single broad diffraction peak of Ni indicates the amorphous structure within the coating. The incorporation of boron in the coating during plating impedes crystallization, for coating with >5 wt% boron, thus the structure appears X-ray amorphous [7, 17]. After heat treatment, the number of characteristic peaks increased compared to those for as-plated coating, and also, the width of the peaks decreased. These results suggested that after heat treatment the coatings were crystallized and precipitated in the nickel boride phases, Ni_2B and Ni_3B. The formation of the nickel boride phases after heat treatment was determined by the boron content of the electroless Ni-B coating [17, 25]. Vitry et al. [17] reported that only Ni_3B phase formed in Ni-B coating when boron content was less than 6 wt%, while Ni_2B phase started to form when the boron content exceeds 6 wt% after heat treatment. Their finding agrees well with the results in this work.

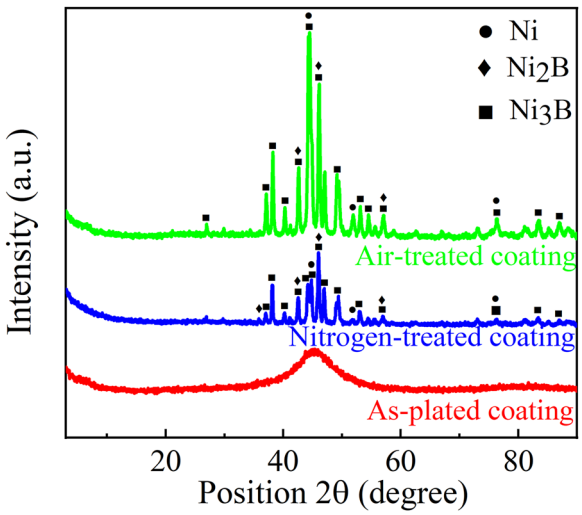

Figure 2 XRD pattern of as-plated electroless Ni-B coating and Ni-B coatings heat-treated in air and nitrogen atmospheres

3.2 Mechanism of the Exoskeleton Arm Surface Properties of Electroless Ni-B Coatings

Figure 3 shows the surface images of titanium alloy and its Ni-B coatings, as well as the cross-sectional image of as-plated Ni-B coating. Consistent with the other studies, the Ni-B coating displayed a typical cauliflower-like texture (Figure 3(b)) [26, 27]. After heat treatment, the cauliflower-like texture could still be observed on the surface of the samples (Figure 3(c, d)). The surface morphology is related to the growth mode of electroless Ni-B coating. As shown in Figure 3(e), the deposition begins with the formation of nodules that grow in a columnar morphology [28]. The cross-section of as-plated coating showed that the substrate was tightly coated with a coating thickness of ~25 μm. The surface roughness of these samples is presented in Table 2. The roughness of titanium alloy was the lowest (measured after grinding by sandpaper,

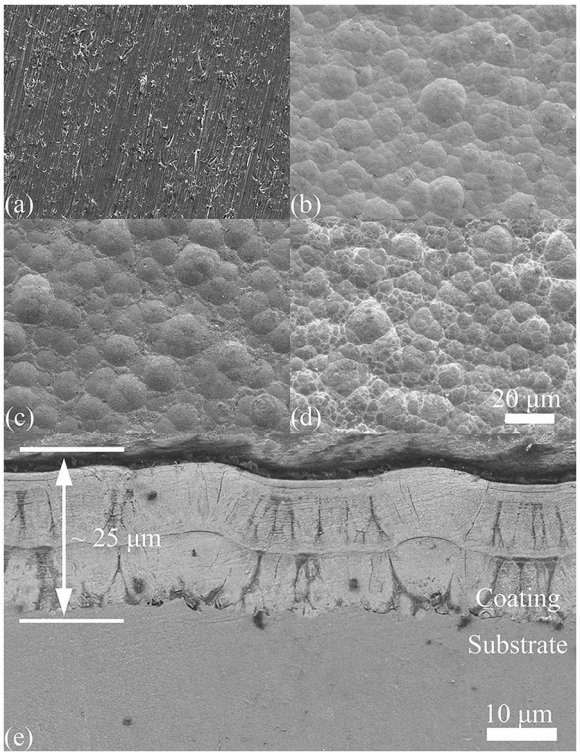

Figure 3 SEM images of the surface of (**a**) TC4 titanium alloy substrate, (**b**) as-plated Ni-B coating, (**c**) air-treated Ni-B coating, (**d**) nitrogen-treated Ni-B coating and (**e**) the cross-section of the as-plated electroless Ni-B coating after etching by 2% nital solution

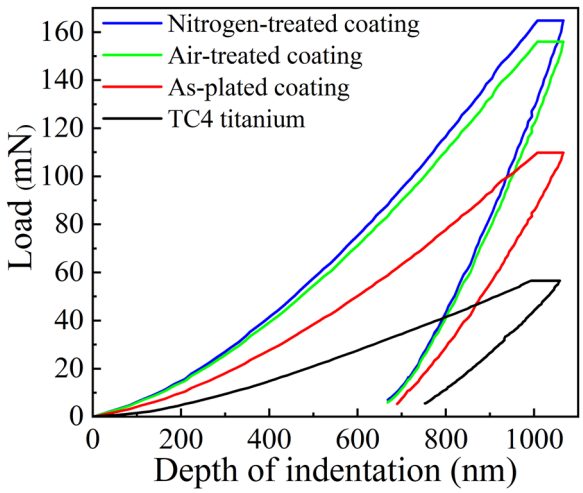

Figure 4 Load–displacement curves for TC4 titanium alloy and its three Ni-B coatings as obtained by nanoindentation at the maximum indentation depth of ~1 μm

prior to the pre-treatment process), followed by those of as-plated, nitrogen-treated, and air-treated coatings, respectively. A significant increase in surface roughness of Ni-B coating after heat treatment was due to grain growth during the heat treatment process [13, 14].

3.3 Mechanical Properties of Electroless Ni-B Coatings

Nanoindentation tests were performed to measure the mechanical properties of the titanium alloy and its Ni-B coatings. Figure 4 shows the typical load-displacement curves of four kinds of samples obtained by nanoindentation. The average nano-hardness and elastic modulus by 20 nanoindentation measurements are shown in Table 2.

The nano-hardness and elastic modulus were calculated using the well-known Oliver-Pharr method [29]. In addition, the micro-hardness of these samples was measured by a Vickers indenter, and the results are also shown in Table 2. It is clear from Table 2 that a significant increase in mechanical properties was observed as a result of heat treatment. The XRD results from Figure 2 provide evidence of crystallization for the explanation of changes in mechanical properties. The amorphous structure of as-plated coating is less packed as compared with that in crystallized phases in heat-treated coatings, there resulting in a lower hardness. Notably, both the nano-hardness and micro-hardness of the three Ni-B coatings were 1–2 times higher than that of titanium alloy, revealing the excellent mechanical properties of Ni-B coatings. Although heat treatment further improved the hardness of as-plated Ni-B coating, it hardly affected the elastic modulus of Ni-B coating. Moreover, creep was observed in the load-displacement curves of all the samples, wherein the creep displacement at the peak load was 64.9 nm for TC4 titanium alloy, 59.2 nm for as-plated coating, 58.9 nm nitrogen-treated coating, and 57.7 nm for air-treated coating. These results indicate that the three Ni-B

Table 2 The surface roughness and mechanical properties of TC4 titanium alloy substrate and its Ni-B coatings

	Roughness (nm)	Micro-hadness (HV)	Nano-hardness (GPa)	Modulus (GPa)
TC4	76.7 ± 5.7	303.5 ± 28.9	3.4 ± 0.4	101.8 ± 5.4
As-plated coating	364.7 ± 25.9	648.5 ± 77.9	7.0 ± 1.0	106.2 ± 6.1
Air-treated coating	717.2 ± 33.8	951.0 ± 84.1	9.8 ± 0.5	109.3 ± 8.9
Nitrogen-treated coating	629.7 ± 80.2	1077.9 ±106.0	12.2 ± 1.2	113.9 ± 10.5

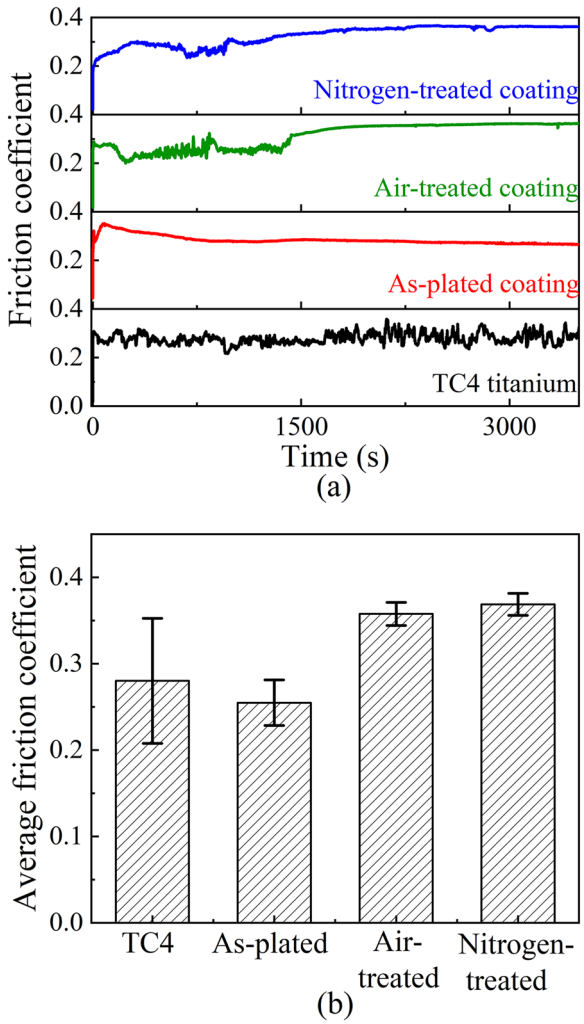

Figure 5 (**a**) The evolution of friction coefficients and (**b**) the average friction coefficients of TC4 titanium alloy substrate and three Ni-B coatings

coatings had better creep resistance than titanium alloy. Moreover, the binding force between the as-plated Ni-B coating and titanium alloy was detected as high as 10.4 N by ramping load scratching test. It reveals that, profiting from our new pre-treatment process, the electroless Ni-B coating was firmly deposited on the surface of titanium alloy, even if titanium alloy was a difficult-to-plate metal.

4 Result and Discussion in Tribological Behaviors

4.1 Friction Properties of Titanium Alloy and Its Ni-B Coatings

The evolution of friction coefficients of titanium alloy and its Ni-B coatings as obtained by rubbing against the Al_2O_3 ball are presented in Figure 5(a). The friction coefficient of titanium alloy shows a clear fluctuation, it is related to its severe wear process [30]. The friction coefficients of Ni-B coatings are relatively stable, but some run-in processes can be observed in the early stage. The run-in process was only ~90 s for the as-plated coating, but it became much longer for both the heat-treated coatings. The process was ~1400 s and ~1000 s for air-treated and nitrogen-treated coatings, respectively. It indicates that the as-plated coating attains stable wear process more easily than the other two heat-treated coatings. The steady average friction coefficients of titanium alloy and its coatings are displayed in Figure 5(b). The friction coefficient of as-plated coating was the lowest at 0.25; thus, as-plated Ni-B coating reduced the friction coefficient of titanium alloy. After heat treatment in air and nitrogen atmospheres, the friction coefficients of the coatings were increased to ~0.35. The difference in steady friction coefficients is mainly related to the different wear mechanisms between samples, which will be discussed in detail in the next sections.

4.2 Enhanced Wear Resistance of Ni-B Coating

As shown in Figure 6(a), after the wear test, optical profilometry images of wear tracks on titanium alloy and its Ni-B coatings were scanned via white light scanning profilometry. Accordingly, the wear volume of these samples was estimated from the cross-sectional profile lines of these tracks (Figure 6(b)). The width and depth of the wear track in titanium alloy were more than those for the Ni-B coatings, wherein the width was 5–6 times larger while the depth was 4–7 times greater than those of the Ni-B coatings. The estimated wear volume of titanium alloy was 19.89×10^{-3} mm^3, while those of as-plated, air-treated, and nitrogen-treated coatings were 0.41×10^{-3} mm^3, 0.99×10^{-3} mm^3, and 0.74×10^{-3} mm^3, respectively. Following electroless plating, the wear volume of titanium alloy was reduced by 96.42%. All the wear track depths for the three electroless Ni-B coatings were less than 4 μm, indicating that the coatings were not completely removed by sliding wear (~25 μm thickness in Ni-B coating). Figure 7 shows the SEM images of wear track in the titanium alloy and three Ni-B coatings. The wear track in the titanium alloy was rougher than in the three Ni-B coatings, along with clear wear grooves and adhesive spots (see the right image of Figure 7(a)). In contrast to the titanium alloy, the wear track in the as-plated Ni-B coating was smoother with some fine grooves along the sliding direction, as shown in Figure 7(b). Different from the as-plated coating, several delamination and micro-cracks appeared within the wear tracks of both air-treated and nitrogen-treated Ni-B coatings. For the heat-treated coatings, the coating is of higher

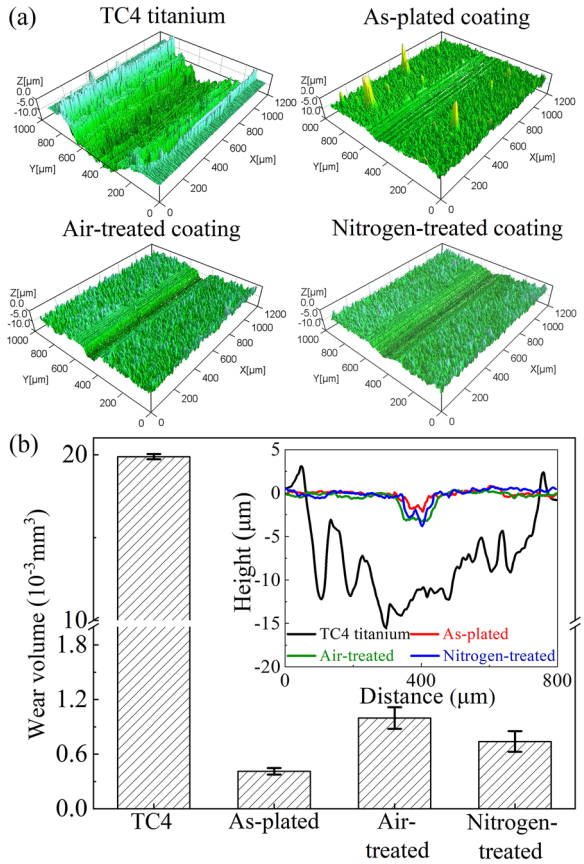

Figure 6 (**a**) Optical profilometry images of wear tracks and (**b**) the corresponding wear volume in TC4 titanium alloy and its three Ni-B coatings, wherein the inset in (**b**) shows the cross-sectional profile lines of wear tracks in (**a**)

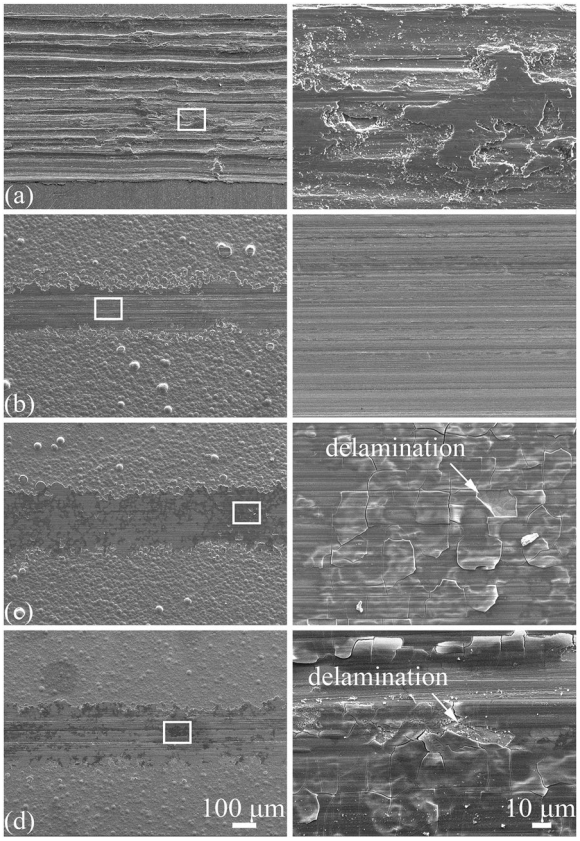

Figure 7 SEM images of the wear track in (**a**) TC4 titanium alloy substrate, (**b**) as-plated coating, (**c**) air-treated coating, and (**d**) nitrogen-treated coating (The images on the right line are enlarged SEM images within the white box of images on the left line)

hardness but simultaneous greater brittleness due to crystallization of the structure. The greater brittleness is confirmed by the long radial-like cracks throughout the coating surface. Similar conclusion on the brittleness due to heat treatment was also given elsewhere [31]. Upon the reciprocating sliding contact, the deformation is readily accompanied by the formation of micro-cracks. As the reciprocating cycle increases, these micro-cracks are prone to merge into a net and eventually lead to the delamination of the deformed materials. In contrast, the as-plated coating exhibits a smooth wear track, in which the micro-cutting grooves can be evidently observed. Unlike the coating in heat-treated coatings which is vulnerable to cracking under friction shear stress, the coating in as-plated coating can undergo the wear process through plastic deformation. This is because the as-plated coating can relieve the friction shear stress effectively by accommodating the strain through plastic deformation due to its high toughness, thereby avoiding the stress concentration on the front of a propagating micro-crack.

Figure 8 displays the optical images and cross-sectional profile lines of the wear scars on the counterbody Al_2O_3 balls after rubbing against titanium alloy and three Ni-B coatings. The sliding track length on Al_2O_3 balls rubbed against titanium alloy was significantly longer and the surface is rougher than those obtained after rubbing against three Ni-B coatings. There were no significant differences in the sizes of wear scars (sliding track length) on the Al_2O_3 balls rubbed against the three Ni-B coatings. However, more wear particle adhesion was observed on the Al_2O_3 balls when rubbed against the heat-treated coatings than when rubbed against as-plated coating. The cross-sectional profile lines in Figure 8(b) show that both the counterbodies rubbed against titanium alloy and heat-treated coatings had material loss, as indicated by a few sunken profile lines at the location of wear scars. However, for the Al_2O_3 balls rubbed against as-plated coating, the cross-sectional profile line was convex at the

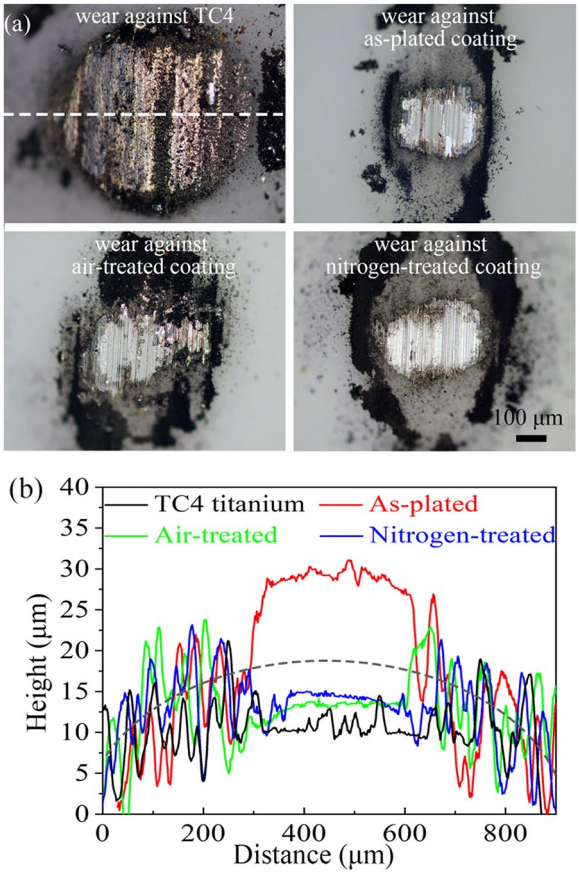

Figure 8 (**a**) The optical images of the wear scars on the Al_2O_3 balls after rubbing against TC4 titanium alloy and its Ni-B coatings, and (**b**) the corresponding cross-sectional profile lines of the Al_2O_3 balls in (**a**) (The white dashed line in (**a**) is the location of the cross-sectional profile lines, which is perpendicular to the sliding direction, and the gray dashed line in (**b**) is the schematic profile line of the non-wear Al_2O_3 ball's surface)

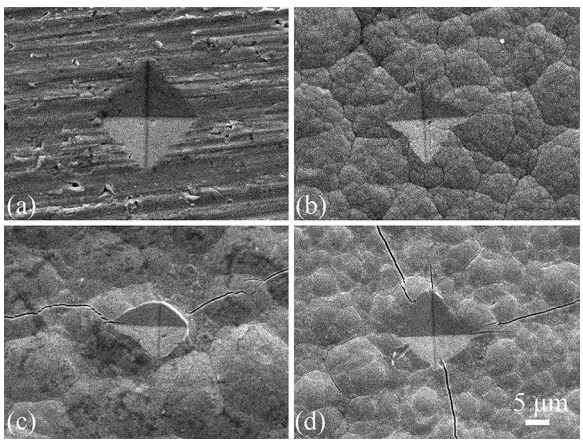

Figure 9 SEM images of micro-indentation impress on (**a**) TC4 titanium alloy substrate, (**b**) as-plated coating, (**c**) air-treated coating, and (**d**) nitrogen-treated coating under the load of 100 g

location of wear scars, which suggests that a tribolayer was transferred on the surface of counterbody.

The higher wear volume of titanium alloy and longer sliding track length of its counterbody Al_2O_3 balls indicate the more serious wear of titanium alloy/ Al_2O_3 ball pair than the Ni-B coatings/ Al_2O_3 ball pairs. In other words, electroless Ni-B coatings greatly improved the wear resistance of titanium alloy. Moreover, the wear mechanism of titanium alloy is different from its three Ni-B coatings. For titanium alloy/ Al_2O_3 ball pair, owing to low hardness and high flow plasticity of titanium alloy, some material build-up occurred on both sides of the wear track in titanium alloy. Combined with the obvious adhesive spots in the wear track of titanium alloy (Figure 7(a)) and rougher wear scar on the Al_2O_3 ball, it reveals that visible adhesive wear occurred on the titanium alloy's surface, which is consistent with other tribological investigations of titanium alloys [32, 33]. Also, the fluctuations in the friction coefficient of titanium alloy (Figure 5) concurs with the characteristics of severe adhesive wear [30]. However, the wear track in the as-plated Ni-B coating is smoother with some fine grooves, signifying that the Ni-B coating is primarily abrasive wear. The high hardness of Ni-B coating greatly resisted wear rubbing by Al_2O_3 ball, which transformed the wear mechanism from the adhesive wear on titanium alloy to the abrasive wear on the as-plated Ni-B coating.

No disastrous fracture or brittle exfoliation was observed during the wear process of the as-plated Ni-B coating. This observation reveals another key information that the electroless Ni-B coating could be firmly deposited on the surface of titanium alloy via the pre-treatment method proposed in this work, even though the coating suffered from strong reciprocating friction. As a difficult-to-plate metal, the titanium alloy was successfully coated by the electroless Ni-B plating along with the display of excellent tribological performance, which would further extend the practical applications of titanium alloys in the engineering fields.

4.3 Effect of Heat Treatment on the Wear Resistance of Electroless Ni-B Coating

The results presented in Table 2 and Figure 4 indicate that heat treatment improved the hardness of electroless Ni-B coatings. Although featuring a higher hardness, the heat-treated coatings showed a lower wear resistance in comparison to the as-plated coating (as shown in Figure 6). This is ascribed to the increased brittleness resulting from the transformation from amorphous to crystallized structure and precipitation of nickel boride phases as a result of heat treatment. Similar conclusion was also given elsewhere [31]. The increase in brittleness will facilitate the micro-crack

nucleation [34], as verified by the long radial-like cracks throughout the coating surface in Figure 9. Owing to the accumulation of dislocation under alternating shear stress, the micro-cracks were readily initiated and propagated along the grain boundaries within the Ni-B coating [5, 35]. Therefore, the modified structure and accumulated thermal stress in the Ni-B coatings following heat treatment resulted in the micro-cracks and delamination of coatings during the reciprocating friction (Figure 7(c, d)). Under the frictional shearing, the exfoliated coating chips became wear particles which got transferred to the surface of Al_2O_3 ball and scattered around the wear scars (Figure 8(a)). The brittleness was significant increased due to heat treatment by leading to the crystallization of amorphous structure of as-plated coating. Under reciprocating sliding wear, the brittle heat-treated coatings are prone to micro-crack nucleation and propagation, causing to the delamination of coating, while the as-plated coating with a high toughness can relieve the friction shear stress effectively by accommodating the strain through plastic deformation, avoiding the stress concentration on the front of a propagating micro-crack. Moreover, the amorphous structure and better ductility of the as-plated coating, the coating material could be removed by ploughing or scratching from the asperities. The removed materials were accumulated and adhered to the wear scar of Al_2O_3 ball to form a tribolayer (Figure 8(b), convex cross-sectional profile line). This tribolayer weakened the shear stress to prevent the Ni-B coating and Al_2O_3 ball from wear. Therefore, the as-plated coating features a higher wear resistance than the heat-treated coating. These results also reveal the reason for the heat-treated coatings having higher friction coefficients with stronger fluctuations relative to the as-plated coating (Figure 5).

Furthermore, the difference in tribochemical reactions may be another reason for the worse wear resistance of heat-treated Ni-B coatings relative to as-plated coating. Figure 10 shows the elemental content of non-wear surface of Ni-B coatings and their wear tracks, as well as the elemental content at the center of wear scars on the Al_2O_3 balls after rubbing against the three Ni-B coatings. As per the results from Figure 10(a), there was much higher O content in the wear tracks as compared to their non-wear surface, indicating the possible oxide wear of Ni-B coating. Moreover, a higher O content was found in the wear tracks of heat-treated coatings than that of the as-plated coating. This result implies that, as compared to the as-plated coating, more severe oxidation wear may occur in the heat-treated coatings, which will be further proved by XPS analysis in Figure 11. Moreover, higher nickel content was found on

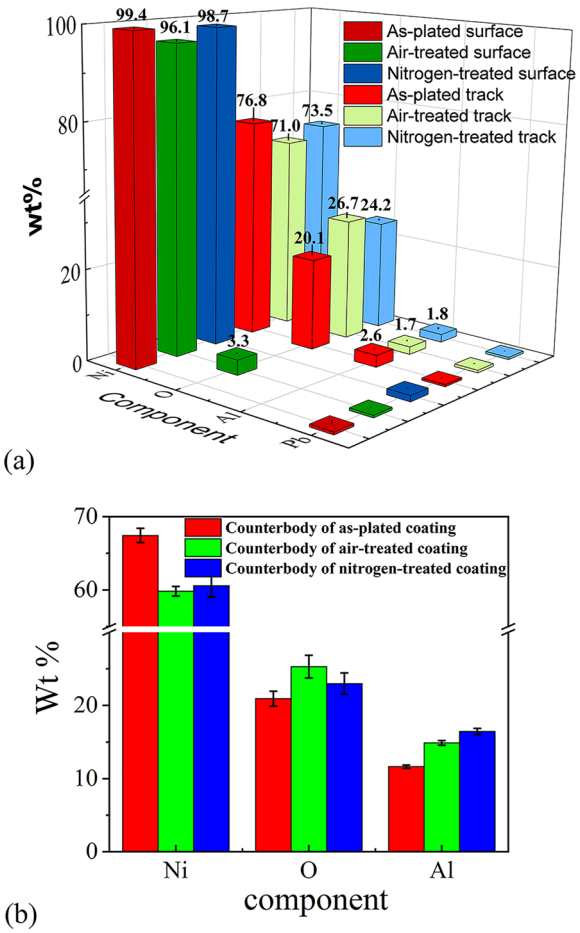

Figure 10 Elemental content of (**a**) the non-wear surface of Ni-B coatings and the wear tracks, and (**b**) of the wear scars on the Al_2O_3 balls after rubbing against three Ni-B coatings, as detected by EDS

the counterbody rubbing against as-plated coating, further proving that more coating material was transferred to the surface of counterbody, to form a tribolayer, as shown in Figure 8.

To verify the formation of oxide during wear, XPS analysis was performed on the wear track of Ni-B coatings after rubbing against Al_2O_3 ball. Figure 11 displays the oxygen 1s, nickel 2p and boron 1s spectra [36] of wear tracks in the three Ni-B coatings. As per the oxygen 1s spectra, Al_2O_3, NiO, B_2O_3 and $Ni(OH)_2$ were found on the surface of wear tracks for all the three Ni-B coatings. Herein, Al_2O_3 is from transferred material on the alumina counter-surface, while B_2O_3, NiO, and $Ni(OH)_2$ are the oxidation products formed during the wear process. As per the nickel 2p and boron 1s spectra, NiO, $Ni(OH)_2$ and B_2O_3 were found, which further verifies the occurrence of oxidation wear of Ni-B coating. In the oxygen 1s spectra, after excluding the impact of Al_2O_3, the area of O peak was largest for the air-treated coating, followed

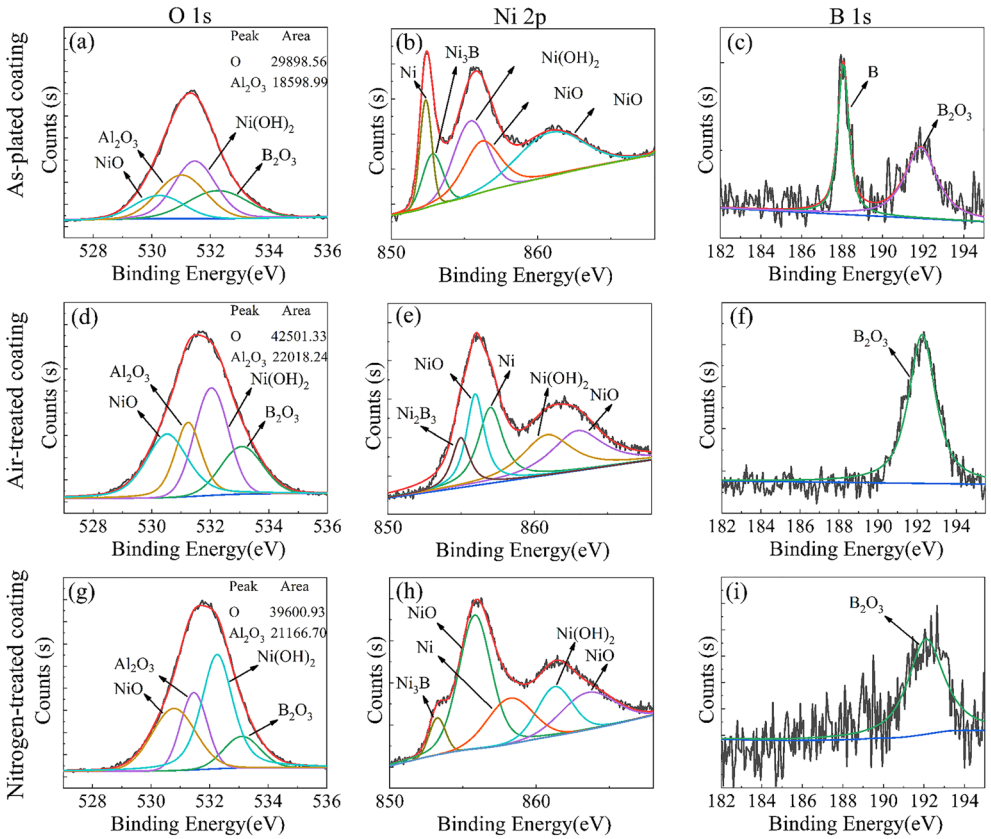

Figure 11 The XPS spectra of O 1s (**a**, **d**, **g**), Ni 2p (**b**, **e**, **h**) and B 1s (**c**, **f**, **i**) of wear tracks in the as-plated coating (**a**–**c**), the air-treated coating (**d**–**f**), and the nitrogen-treated coating (**g**–**i**) after rubbing against alumina ball

by nitrogen-treated coating and as-plated coating. The XPS results are in good agreement with the results of EDS shown in Figure 10(a). All the XPS and EDS results further verify that as compared to the as-plated coating, more severe oxidation wear occurred in the heat-treated coatings. On the one hand, the relatively severe oxidation of heat-treated can be attributed to higher friction temperatures produced during the wear process because of greater friction coefficients. On the other hand, the larger wear scar on the heat-treated coatings (see Figure 6) provides greater chance of reacting between coating and oxygen, making the more severe oxidation of heat-treated coatings than as-plated coating.

Moreover, in the B 1s spectra of the wear track for the as-plated coating (Figure 11(c)), there are two peaks, where the peak at 188 eV corresponds to elemental B and the peak at 192 eV is related to boron oxide compound. However, in the B 1s spectra of the heat-treated coatings, there is only one peak at 192 eV (Figure 11(f) and (i)). It thus indicates that there is still some unoxidized boron element in the as-plated coating, but the boron in the wear track of the heat-treated coatings has been completely oxidized. It further verified that the oxidative wear of the heat-treated coatings is more severe than that of the as-plated coating.

As shown in the oxygen 1s spectra in Figure 11, for each sample, the contribution including NiO and $Ni(OH)_2$ is significantly larger than that of B_2O_3. It reveals that the reaction between Ni and O is the more dominant oxidation than the reaction between B and O. Moreover, the area of oxide peak including NiO and $Ni(OH)_2$ was 48953.03 for air-treated coating, 48891.31 for the nitrogen-treated coating, and 21123.14 for the as-plated coating. The more oxidation product, nickel oxide, led to the intergranular embrittlement of heat-treated Ni-B coating [37]. Under cyclic shear stress, the decohesive nickel oxide particles became wear particles at the frictional interface of coating and Al_2O_3 ball and aggravate the wear. Briefly, more severe oxidation accompanied with more production of nickel oxide during the wear process was one of the reasons for the worse wear resistance of heat-treated Ni-B coatings than as-plated coating.

Comparing the wear tracks on the air-treated and nitrogen-treated coatings, the SEM image in Figure 7 displays that there was no significant difference in the damage mode. Besides, the EDS results in Figure 10(a)

demonstrate that there were no significant differences in the chemical component concentration of the two heat-treated coatings. As shown in Figure 5, the friction coefficients of two heat-treated coatings were not substantially different. All the results reveal that the heat treatment atmosphere barely affected the tribological behavior of the electroless Ni-B coating. The minuscule difference in the wear volume (Figure 6(b)) can be attributed to differences in the hardness of two coatings treated in air and nitrogen atmospheres.

5 Conclusions

In this work, the electroless Ni-B coating was successfully deposited on the TC4 titanium alloy's surface using a new pre-treatment process. The coated samples were further heat-treated in air and nitrogen atmospheres. The tribological properties of titanium alloy and its electroless Ni-B coatings were comparatively investigated based on these treatments. The main conclusions from these experimental results are summarized below.

(1) The mechanical properties of the electroless Ni-B coating were enhanced by the heat treatment, where the heat-treated coating in nitrogen has a higher hardness. This is ascribed to the structural evolution from amorphous to crystallized structure due to heat treatment and a higher fraction of nickel boride phases in coatings heat-treated in nitrogen than those heat-treated in air.
(2) The heat-treatment deteriorates the wear resistance of as-plated Ni-B coating by increasing the brittleness significantly. The crystallization of amorphous structure is the main reasons for the increased brittleness, which leads to delamination of wear debris and thus a low wear resistance. More severe oxidation combined with higher tribochemical production of nickel oxide modified the wear mechanism of heat-treated Ni-B coatings.
(3) Both the air-treated and nitrogen-treated coatings show almost the same friction coefficient and damage mode in wear response, indicating the same wear mechanism in reciprocating sliding contact.

Acknowledgements
Not applicable.

Authors' Contributions
JY conceived and directed the work, and YJ and JL conducted and analyzed the experiments with support by HQ, YZ and HH. All authors read and approved the final manuscript.

Funding
Supported by Sichuan Provincial Science and Technology Program of China (Grant No. 2018JY0245), National Natural Science Foundation of China (Grant No. 51975492), and Natural Science Foundation of Southwest University of Science and Technology of China (Grant No. 19xz7163).

Declarations

Competing Interests
The authors declare no competing financial interests.

Received: 30 May 2021 Revised: 29 April 2022 Accepted: 4 January 2024
Published online: 23 February 2024

References

[1] Xiaoliang Liang, Zhanqiang Liu, Bing Wang. State-of-the-art of surface integrity induced by tool wear effects in machining process of titanium and nickel alloys: A review. *Measurement*, 2019, 132: 150–181.
[2] L Wagner. Mechanical surface treatments on titanium, aluminum and magnesium alloys. *Mater. Sci. Eng. A-Struct. Mater. Prop. Microstruct. Process*, 1999, 263: 210–216.
[3] Fei Weng, Chuanzhong Chen, Huijun Yu. Research status of laser cladding on titanium and its alloys: A review. *Mater. Des.*, 2014, 58: 412–425.
[4] A Bloyce, P H Morton, T Bell. Surface engineering of titanium and titanium alloys. *Surface Engineering*, 1994: 835–851.
[5] Sepehr Yazdani, Mahboubi Farzad. Comparison between microstructure, wear behavior, and corrosion resistance of plasma-nitrided and vacuum heat-treated electroless Ni–B coating. *Journal of Bio- and Tribo-Corrosion*, 2019, 5: 1–11.
[6] T S N Sankara Narayanan, S K Seshadri. Formation and characterization of borohydride reduced electroless nickel deposits. *J. Alloy. Compd.*, 2004, 365: 197–205.
[7] K Krishnaveni, T S N Sankara Narayanan, S K Seshadri. Electroless Ni–B coatings: preparation and evaluation of hardness and wear resistance. *Surf. Coat. Technol.*, 2005, 190: 115–121.
[8] Esteban Correa, Zuleta Alejandro Alberto, Guerra Laura, et al. Tribological behavior of electroless Ni–B coatings on magnesium and AZ91D alloy. *Wear*, 2013, 305: 115–123.
[9] Sandra Arias, Castaño Juan G, Correa Esteban, et al. Effect of heat treatment on tribological properties of Ni-B coatings on low carbon steel: Wear maps and wear mechanisms. *Journal of Tribology*, 2019, 141: 091601-091609.
[10] V Vitry, F Delaunois. Formation of borohydride-reduced nickel–boron coatings on various steel substrates. *Applied Surface Science*, 2015, 359: 692–703.
[11] J A Santiago, I Fernández-Martínez, A Wennberg, et al. Adhesion enhancement of DLC hard coatings by HiPIMS metal ion etching pretreatment. *Surf. Coat. Technol.*, 2018, 349: 787–796.
[12] Rasid Ahmed Yildiz, Genel Kenan, Gulmez Turgut. Effect of heat treatments for electroless deposited Ni-B and Ni-W-B coatings on 7075 Al alloy. *Int. J. Mater. Mech. Manuf.*, 2017, 5: 83–86.
[13] Arkadeb Mukhopadhyay, Barman Tapan Kumar, Sahoo Prasanta. Effects of heat treatment on tribological behavior of electroless Ni–B coating at elevated temperatures. *Surf. Rev. Lett.*, 2018, 25: 1850014.
[14] Yazdan Shajari, Alizadeh Asad, Seyedraoufi Zahra Sadat, et al. The effect of heat treatment on wear characteristics of nanostructure Ni-B coating on marine bronze. *Mater. Res. Express.*, 2019, 6: 105040.
[15] Véronique Vitry, Kanta Abdoul-Fatah, Delaunois Fabienne. Application of nitriding to electroless nickel–boron coatings: Chemical and structural effects; mechanical characterization; corrosion resistance. *Mater. Des.*, 2012, 39: 269–278.
[16] S Yazdani, R Tima, F Mahboubi. Investigation of wear behavior of as-plated and plasma-nitrided Ni-B-CNT electroless having different CNTs concentration. *Appl. Surf. Sci.*, 2018, 457: 942–955.
[17] V Vitry, L Bonin. Increase of boron content in electroless nickel-boron coating by modification of plating conditions. *Surf. Coat. Technol.*, 2017, 311: 164–171.
[18] F Mindivan, H Mindivan, C Darcan. Electroless Ni–B coating of pure titanium surface for enhanced tribocorrosion performance in artificial saliva and antibacterial activity. *Tribol. Ind.*, 2017, 39: 270–276.

[19] Bonin Luiza, Véronique Vitry, Fabienne Delaunois. Influence of the anionic part of the stabilizer on electroless nickel-boron plating. *Mater. Manuf. Process*, 2017, 33: 227–231.
[20] R Grzeschik, D Schafer, T Holtum, et al. On the overlooked critical role of the pH value on the kinetics of the 4-nitrophenol NaBH4-reduction catalyzed by noble-metal nanoparticles (Pt, Pd, and Au). *J. Phys. Chem. C*, 2020, 124: 2939–2944.
[21] A Salicio-Paz, A Dalmau, H Grande, et al. Impact of the multilayer approach on the tribocorrosion behaviour of nanocrystalline electroless nickel coatings obtained by different plating modes. *Wear*, 2020, 456: 203384.
[22] Robert J K Wood. Tribo-corrosion of coatings: A review. *Journal of Physics D: Applied Physics*, 2007, 40: 5502–5521.
[23] Arkadeb Mukhopadhyay, Barman Tapan Kumar, Sahoo Prasanta. Friction and wear performance of electroless Ni-B coatings at different operating temperatures. *Silicon*, 2018, 11: 721–731.
[24] Huimin Qi, Wen Hu, Hongtu He, et al. Quantitative analysis of the tribological properties of phosphate glass at the nano-and macro-scales. *Friction*, 2020: 1–12.
[25] J R López, P F Méndez, J J Pérez-Bueno, et al. The effect of boron content, crystal structure, crystal size on the hardness and the corrosion resistance of electrodeposited Ni-B coatings. *Int. J. Electrochem. Sci.*, 2016, 11: 4231–4244.
[26] R A Shakoor, Kahraman Ramazan, Wei Gao, et al. Synthesis, characterization and applications of electroless Ni-B coatings-A review. *Int. J. Electrochem. Sci.*, 2016, 11: 2486–2512.
[27] E Duru, F Dogan, M Uysal, et al. Optimization of Ni-B coating bath and effect of DMAB concentration on hardness and wear. *Surf. Interfaces*, 2021, 22: 100880.
[28] U Matik. Improvement of surface properties of iron based powder metal compacts by electroless Ni-B coating. *J. Fac. Eng. Archit. Gazi Univ.*, 2018, 33: 1603–1610.
[29] V Morar, C Pyrtsac, N Curmei, et al. Nanoindentation of ZnSnO/Si thin films prepared by aerosol spray pyrolysis. *Rom. J. Phys.*, 2021, 66: 1–18.
[30] İlhan Çelik, Karakan Mehmet, Bülbül Ferhat. Investigation of structural and tribological properties of electroless Ni–B coated pure titanium. *Proc. Inst. Mech. Eng. Part J.-J. Eng. Tribol.*, 2015, 230: 57–63.
[31] M Franco, W Sha, V Tan, et al. Insight of the interface of electroless Ni-P/SiC composite coating on aluminium alloy, LM24. *Materials & Design*, 2015, 85: 248–255.
[32] M Lepicka, M Gradzka-Dahlke, I Zaborowska, et al. Recurrence analysis of coefficient of friction oscillations in DLC-coated and non-coated Ti6Al4V titanium alloy. *Tribology International*, 2022, 165: 107342.
[33] M Bogdan-Chudy, P Nieslony, M K Gupta, et al. Tribological and thermal behavior with wear identification in contact interaction of the Ti6Al4V-sintered carbide with AlTiN coatings pair. *Tribology International*, 2022, 167: 107394.
[34] Vaibhav Nemane, Chatterjee Satyajit. Scratch and sliding wear testing of electroless Ni–B–W coating. *Journal of Tribology*, 2019, 142: 021705.
[35] X T Song, X H Shi, Z H Xia, et al. Effects of Ni-P coating on mechanical properties of Al0.3CoCrFeNi high-entropy alloys. *Materials Science and Engineering a-Structural Materials Properties Microstructure and Processing*, 2019, 752: 152–159.
[36] NIST X-ray Photoelectron Spectroscopy Database. NIST Standard Reference Database Number 20. National Institute of Standards and Technology. Gaithersburg MD. 2000. Accessed 11 July 2020. https://srdata.nist.gov/xps/.
[37] David A Woodford. Gas phase embrittlement and time dependent cracking of nickel based superalloys. *Energy Materials*, 2006, 1: 59–79.

Yao Jia born in 1997, is currently a master candidate at *Key Laboratory of Testing Technology for Manufacturing Process in Ministry of Education, State Key Laboratory of Environment-friendly Energy Materials, Southwest University of Science and Technology, China*.

Jianping Lai born in 1985, is currently a lecturer at *Key Laboratory of Testing Technology for Manufacturing Process in Ministry of Education, State Key Laboratory of Environment-friendly Energy Materials, Southwest University of Science and Technology, China*. He received his doctorate degree from *Central South University, China*, in 2019.

Jiaxin Yu born in 1982, is currently a professor, a doctoral supervisor at *Key Laboratory of Testing Technology for Manufacturing Process in Ministry of Education, State Key Laboratory of Environment-friendly Energy Materials, Southwest University of Science and Technology, China*. He received his doctorate degree from *Southwest Jiaotong University, China*, in 2011.

Huimin Qi born in 1986, is currently an associate professor at *Key Laboratory of Testing Technology for Manufacturing Process in Ministry of Education, State Key Laboratory of Environment-friendly Energy Materials, Southwest University of Science and Technology, China*. She received her doctorate degree from *Lanzhou Institute of Chemical Physics, Chinese Academy of Sciences, China*, in 2018.

Yafeng Zhang born in 1983, is currently an associate professor at *Key Laboratory of Testing Technology for Manufacturing Process in Ministry of Education, State Key Laboratory of Environment-friendly Energy Materials, Southwest University of Science and Technology, China*. He received his doctorate degree from *Southwest Jiaotong University, China*, in 2015.

Hongtu He born in 1988, is currently an associate professor at *Key Laboratory of Testing Technology for Manufacturing Process in Ministry of Education, State Key Laboratory of Environment-friendly Energy Materials, Southwest University of Science and Technology, China*. He received his doctorate degree from *Southwest Jiaotong University, China*, in 2015.